



Adsorptive remediation of Cu(II) and Cd(II) contaminated water using manganese nodule leaching residue

N.S. Randhawa^{a,*}, N.N. Das^b, R.K. Jana^a

^aMetal Extraction & Forming Division, CSIR-National Metallurgical Laboratory, Jamshedpur 831007, Jharkhand, India

Tel. +91 657 2345184; Fax: +91 657 2345245; email: nsrandhawa@gmail.com

^bDepartment of Chemistry, North Orissa University, Baripada 757003, Odisha, India

Received 7 February 2013; Accepted 28 April 2013

ABSTRACT

Investigations carried out for the application of manganese nodule leaching residue in the removal of Cu(II) and Cd(II) from aqueous solution by adsorption are described. Several parameters, namely pH of solution, time, initial concentration of adsorbate metal ion, residue dose, etc., have been varied to study the feasibility of using residue as potential adsorbent for remediation of Cu(II) and Cd(II) contaminated water. The adsorption kinetics followed pseudo-second-order equation and the rate of adsorption increased with solution temperature. The equilibrium data was best fitted into Langmuir adsorption isotherm and the maximum adsorption capacities of washed manganese nodule residue (*w*MNR) towards Cu(II) and Cd(II) were found to be 26.95 and 32.26 mg g⁻¹, at pH 5.5 and temperature 303 K, which improved to 40.32 and 38.17 mg g⁻¹, respectively, upon raising the solution temperature to 323 K. Negative values of ΔG° indicated that adsorption of Cu(II) and Cd(II) onto *w*MNR was spontaneous. The activation energy for Cu(II) and Cd(II) adsorption onto *w*MNR ranged between 40 and 65 kJ mol⁻¹. A mixed-type uptake mechanism involving chemical interaction and diffusion inside adsorbent particle is discussed. This study would be useful for future application of this material in the remediation of copper and cadmium contaminated wastewater.

Keywords: Adsorption; Manganese nodules; Manganese nodule leached residue; Heavy metals; Chemisorption

1. Introduction

Effluents from most of the industrial units contain metallic pollutants. Heavy metals present in these effluents, when discharged untreated, pollute water bodies and pose threat to ecosystem. The elevated level of lead and other heavy metals, e.g. cadmium, chromium and mercury, in the local water streams is a

major concern to public health. Mining, electroplating, metal processing, textile industry, and battery industry are the main sources of heavy metal ion contamination. Metals like lead, cadmium, copper, arsenic, nickel, chromium, zinc, and mercury have been recognized as hazardous heavy metals. Heavy metals are nonbiodegradable and tend to accumulate in living organisms, causing various life threatening disorders [1].

*Corresponding author.

Table 1
Permissible limits of copper (Cu) and cadmium (Cd) for discharge into various water bodies and in drinking water [4,5]

Type of water	Permissible limits (mg L ⁻¹)	
	Cu	Cd
Surface water	3.0	2
Public sewer	3.0	1
Marine coastal areas	3.0	2
Drinking water	0.05 ^a	0.01 ^b

^aRelaxable up to 1.5 mg L⁻¹ in absence of alternate source.

^bNo relaxation.

Copper and cadmium are major pollutant in the effluents discharged from electroplating, electrical and electronic, hydrometallurgical processing, ore beneficiation, tanneries, distilleries, etc industries [2]. Copper (Cu) is mined as a primary ore product from copper sulfide and oxide ores. Mining activities are the major source of copper contamination in groundwater and surface waters. Other sources of copper include algicides, chromated copper arsenate pressure-treated lumber, and copper pipes [3]. Cadmium (Cd) occurs naturally in the form of CdS or CdCO₃. Cadmium is recovered as a by-product from the mining of sulfide ores of lead, zinc and copper. Sources of cadmium contamination include plating operations and the disposal of cadmium-containing wastes [3]. The permissible limits for discharge of copper and cadmium into different stream [4] and that in drinking water [5] in India are given in Table 1.

The important technologies available for copper and cadmium removal comprise electrocoagulation, electro flotation, ion exchange, reverse osmosis, adsorption onto activated carbon, etc. [6–8]. Among them, adsorption technique has been viewed as most attractive due to simpler operation and effectiveness [7,8]. In addition, many adsorption techniques regenerate the adsorbent and reduce the operational cost. The key factor for the selection of an adsorbent lies with its adsorption efficiency and most importantly its cost. In addition to the widely studied adsorbents like activated carbon, low-cost bio-sorbents based on agriculture (stems, peels, husks, shells, leaves, etc.), agro-industries' waste materials, calcite, biomass, red-mud, silica gel, and blast furnace sludge have also been tried for the removal of copper and cadmium from wastewater [9–13]. Metallic oxides (Fe, Mn, Al, etc.), especially of waste category, are of much interest due to their

effectiveness towards remediation of heavy metals from contaminated aqueous bodies [11–13].

Residues generated after hydrometallurgical treatment of manganese nodules or polymetallic sea nodules contain oxides/oxy-hydroxides of Fe, Mn, Al, and Si with a reasonable porosity and surface area, which have been utilized as an effective adsorbent for a variety of species [14–16]. Therefore, studies are carried out to investigate the sorption characteristics of residue generated in the reduction-roast ammoniacal leaching of manganese nodules for the removal of Cu(II) and Cd(II) from its aqueous solution. Variables like pH of solution, contact time, temperature, initial adsorbate ion concentration, adsorbent dose, etc. are studied to establish the optimum conditions to achieve maximum loading of Cu(II) or Cd(II) onto leached manganese nodule residue.

2. Materials and methods

2.1. Adsorbent

The manganese nodules residue (MNR) used in present study is collected from one of the large-scale Reduction roasting—Ammonia leaching trials of Indian Ocean manganese nodules, at Council of Scientific & Industrial Research-National Metallurgical Laboratory (CSIR-NML), Jamshedpur, India. The MNR is air-dried before characterization. In order to remove entrapped leach liquor and residual metal ion and ammonia, MNR is washed with water (L) to remove ammonia and metal ions of entrapped leach liquor. For washing, a certain amount of MNR (S) is agitated in a steel vessel with L/S ratio of 10 for 2 h following filtration through a Sparkler filter press and then dried in hot air oven at 110 °C for 8 h. Representative samples of unwashed (MNR) and washed manganese nodule residue (*w*MNR) are collected by conning and quartering method for characterization. The *w*MNR is used as adsorbent in all the adsorption experiments.

2.2. Stock solutions and standards

Accurately weighed 3.821 g of Cu(NO₃)₂·3H₂O is dissolved in 1,000 mL of deionised water to obtain a stock solution of 1,000 mg L⁻¹ of copper. Different concentrations of metal solutions are prepared by dilution of required volume of stock solution. The stock solution (1,000 mg L⁻¹) of cadmium is prepared by dissolving 2.744 g Cd(NO₃)₂·4H₂O in deionised water and the solution is made slightly acidic by adding a few drops of HNO₃ to prevent hydrolysis of Cd(II).

All the chemicals are AR grade and procured from Merck Specialities Pvt. Ltd. India. The water processed by Milli-Q system is used for all the experimental and analytical purposes.

2.3. Equipment and apparatus

The major and minor constituents in unwashed (MNR) and washed (*w*MNR) samples were analyzed by wet chemical methods and by atomic absorption spectroscopy (AAS), respectively. The particle sizes of MNR and *w*MNR were determined using a Malvern Instruments SA-CP3 particle size analyzer. X-ray diffraction patterns were recorded on a Siemens D500 X-ray diffractometer using Cu K α radiation. Surface areas were determined by the BET method using a Quantachrome Nova instrument. Points of zero charge (pH_{PZC}) were determined by batch acid-base titration techniques as reported by Huang and Ostavic [17]. An SD Scientific Ltd., Kolkata make water bath shaker fitted with programmable heating (25–50°C) system and stepless shaking speed was used in all the adsorption experiments. pH adjustments were made with the additions of 0.01 M HNO₃ and 0.01 M NaOH using digital pH-meter (Toshniwal CL54) fitted with a combined glass electrode after calibration with National Bureau of Standards buffers. Copper and cadmium contents in each experiment were determined with AAS (PerkinElmer AAnalyst 400). The absorbance of copper and cadmium were recorded at 237.4 and 232.0 nm, respectively, using individual Hollow Cathode Lamps by aspiration of acidified samples in air-acetylene flame with an integration time of 5 s. Absorbance of each samples was recorded in triplicates and average values were used for all the calculations.

2.4. Adsorption kinetics experiments

For kinetic studies, typically, 50 mL of Cu²⁺ or Cd²⁺ solution at desired concentration (25, 50, 75, and 100 mg L⁻¹) with 50 mg of *w*MNR in 100 mL stoppered conical flask was taken. The required pH was adjusted and was then mechanically shaken (120 strokes min⁻¹) using a water bath shaker, which was maintained at temperatures 303, 313, and 323 K as per requirement. Separate kinetic experiments were performed with solution containing either Cu²⁺ or Cd²⁺ under the above conditions. Samples were withdrawn at certain time interval and the solid adsorbent was separated by filtration. The remaining Cu²⁺ or Cd²⁺ in the filtrate was analyzed by AAS as explained in above section. The amount of Cu²⁺ or

Cd²⁺ adsorbed per gram of the *w*MNR, Q_t (mg g⁻¹) was calculated using Eq. (1).

$$q_e = \frac{(C_o - C_e)V}{W \times 1,000} \quad (1)$$

where q_e , C_o , C_e , V , and W represent the amount of Cu (II) or Cd(II) adsorbed onto the solid at equilibrium (mg g⁻¹), the initial concentration of metal ions (mg L⁻¹), the final equilibrium concentration of metal ions (mg L⁻¹), the volume of the solution (mL), and the amount of adsorbent employed (g), respectively.

2.5. Adsorption isotherms experiments

Six solutions with concentrations 5–100 mg L⁻¹ were made by dilution of stock solutions of both the metal ions (Cu²⁺ and Cd²⁺). pH of the solution was adjusted to 5.5 and 50 mg of *w*MNR was added to 50 ml of each metal solution and agitated for equilibrium time obtained from kinetics experiments. Separate isotherm experiments were carried out for Cu²⁺ and Cd²⁺ adsorption onto *w*MNR. At the end of each experiment, solution is filtered and the filtrate was analyzed for metal ions by AAS as explained above.

2.6. Data evaluation

The kinetic and equilibrium data was analyzed with following models.

2.6.1. Kinetic models:

The adsorption kinetics was evaluated using three models, namely the pseudo-first-order [18], the pseudo-second-order [19], and intraparticle diffusion model [20].

Pseudo-first-order kinetic model: the pseudo-first-order kinetic model (Lagergren's equation) describes adsorption in solid-liquid systems based on the sorption capacity of solids [18]. In this model, it has been assumed that one metal ion is sorbed onto one sorption site on the *w*MNR surface. The linear form of pseudo-first-order model can be expressed in Eq. (2) as:

$$\ln(q_e - q_t) = \ln q_e - k_1 \times t \quad (2)$$

where q_e and q_t (mg g⁻¹) are the adsorption capacities at equilibrium and at time t (h), respectively. The value of k_1 is derived from the slope of the linear plots of $\log(q_e - q_t)$ vs. t .

Pseudo-second-order kinetic model: the pseudo-second-order model assumes that one metal ion is sorbed onto two sorption sites on the *w*MNR surface. This has been applied for analyzing chemisorption kinetics from liquid solutions [19], is linearly expressed in Eq. (3) as:

$$\frac{t}{q_t} = \frac{1}{k_2 q_e^2} + \frac{1}{q_e t} \quad (3)$$

where k_2 is the rate constant for pseudo-second-order adsorption ($\text{g mg}^{-1} \text{h}^{-1}$) and $k_2 q_e^2$ or h ($\text{mg g}^{-1} \text{h}^{-1}$) is the initial adsorption rate. The values of $1/k_2 q_e^2$ and $1/q_e$ are derived from the intercept and slope of the linear plots of t/q_t vs. t , which eventually leads to values of k_2 and q_e (cal.).

Intraparticle diffusion model: the intraparticle diffusion plays important role in adsorption process involving porous materials. Therefore, *w*MNR was also evaluated for the role of intraparticle diffusion during Cu^{2+} and Cd^{2+} adsorption from aqueous solution. The kinetics data was fitted into Intraparticle diffusion model, expressed with the Eq. (4), given by Weber and Morris [20].

$$q_t = k_{id} \times t^{1/2} \quad (4)$$

where q_t is the amount of metal ions adsorbed at time t (mg g^{-1}) and k_{id} is the intraparticle diffusion rate constant ($(\text{mg g}^{-1} \text{min}^{-1/2})$). Value of k_{id} is obtained from the slope of plots between q_t and t .

2.6.2. Isotherm models

The equilibrium data was fitted into the two commonly used isotherm models and goodness of fit was determined on the basis of regression analysis. Those models are described below.

Langmuir model: the simplest known adsorption isotherm was proposed by Langmuir [21], which was based on the theoretical principle that only a single adsorption layer exists on an adsorbent and it represents the equilibrium distribution of metal ions between the solid and liquid phases. The linearized form of the Langmuir equation may be written as:

$$\frac{C_e}{q_e} = \frac{1}{b Q^o} + \frac{C_e}{Q^o} \quad (5)$$

where C_e is equilibrium concentration (mg L^{-1}); q_e is amount adsorbed at equilibrium (mg g^{-1}); b is langmuir isotherm constants related to affinity of adsorbent toward metal ion; and Q^o is adsorption maxima

or adsorption capacity (mg g^{-1}). A plot of $C_e/q_e \approx C_e$ should be linear if adsorption follows Langmuir isotherm. The values of b and Q^o can be calculated by slope and intercept of the straight line.

Freundlich model: the Freundlich adsorption isotherm [22] is an indicator of the extent of heterogeneity of the adsorbent surface. A linear form of this expression, as given below, was used for adsorption data analysis.

$$\ln q_e = (1/n) \ln C_e + \ln K_f \quad (6)$$

where q_e = amount of metal ion sorbed per unit weight of adsorbent, mg g^{-1} ; C_e = equilibrium concentration of metal ion in aqueous solution, mg L^{-1} ; and K_f and $1/n$ stand for empirical constants related to adsorption capacity and intensity, respectively. Values of K_f and n are calculated from the intercept and slope of the plot $\ln q_e$ vs. $\ln C_e$.

2.6.3. Thermodynamics of adsorption

The thermodynamic parameters were determined from the thermodynamic equilibrium constant K_d (or the thermodynamic distribution coefficient) derived from adsorption equilibrium experiments. The standard Gibbs free energy ΔG° (kJ mol^{-1}), standard enthalpy change ΔH° (kJ mol^{-1}), and standard entropy change ΔS° ($\text{J mol}^{-1} \text{K}^{-1}$) were calculated using the following equations [23]:

$$\Delta G^\circ = -RT \ln K_d \quad (7)$$

$$\ln K_d = \frac{\Delta S^\circ}{R} - \frac{\Delta H^\circ}{RT} \quad (8)$$

K_d can be defined as:

$$K_d = \frac{a_s}{a_e} = \frac{\gamma_s C_s}{\gamma_e C_e} \quad (9)$$

where a_s = activity of adsorbed metal ion, a_e = activity of metal ion in solution at equilibrium, γ_s = activity coefficient of adsorbed metal ion, γ_e = activity coefficient of metal ion in equilibrium solution, C_s = metal ion adsorbed on *w*MNR (mg g^{-1}), and C_e = metal ion concentration in solution at equilibrium (mg L^{-1}).

K_d at different temperatures was determined by plotting $\ln(C_s/C_e)$ vs. C_s and extrapolating C_s to zero [23–25]. $\ln K_d$ was plotted against $1/T$ to calculate ΔH° and ΔS° from the slope and intercept, respectively.

Table 2
Chemical analysis of MNR and *w*MNR

Element/radical	Chemical composition, % by mass	
	MNR	<i>w</i> MNR
Mn(T) ^a	25.66	26.11
Mn ²⁺	14.02	13.71
Mn ³⁺	4.87	4.92
Mn ⁴⁺	6.77	7.22
Fe	9.92	10.19
SiO ₂	15.28	16.44
Al ₂ O ₃	3.53	3.54
S	0.37	0.08
NH ₄ ⁺	0.30	Not found
Co	0.035	0.039
Ni	0.07	0.05
Cu	0.26	0.13
Moisture	8.96	6.18
LOI ^b	18.85	17.01

^aTotal Mn content with Mn²⁺, Mn³⁺ and Mn⁴⁺.

^bLOI=loss in weight on ignition.

3. Results and discussion

3.1. Characterisation of adsorbent

The chemical analyses data of MNR and *w*MNR are listed in Table 2. It is evident that the leached residue mainly contained Mn, Fe, Si, and Al. On washing MNR with deionised water, marginal changes in the weight percentages of Mn, Fe, SiO₂, C, CaO, and MgO were noted, while the losses of adsorbed metal ions such as Cu²⁺ and Ni²⁺ along with

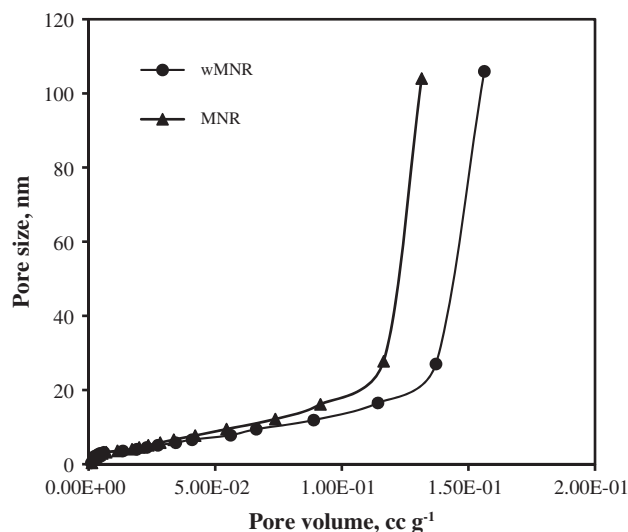


Fig. 1. Pore size distribution of MNR and *w*MNR.

S were quite significant. In a previous study on the morphology of *w*MNR under scanning electron microscope, the shapes of the particles were seen to be irregular and particles were congregated moderately [26]. Particle size analyses showed that the MNR contained very fine particles with mean particle diameters (d_{50}) of 17.8 μm . Significant decrease in particle size was observed in *w*MNR (d_{50} = 11.38 μm). The pore size distribution of MNR and *w*MNR is shown in Fig. 1 depicting wide range of pore width (0.36–106 nm) spanning from micro- (<2 nm), meso- (2–50 nm) to the macro- (>50 nm) pores. The BET surface areas of MNR and *w*MNR were found to be 60.9 and 66.7 m^2/g , respectively. The marginally higher surface area of *w*MNR was presumably due to an increased number of accessible pores on washing adsorbed species out from MNR. The other possible reason could be comparatively lower particle size of *w*MNR than that of MNR. The pH_{PZC} of *w*MNR was

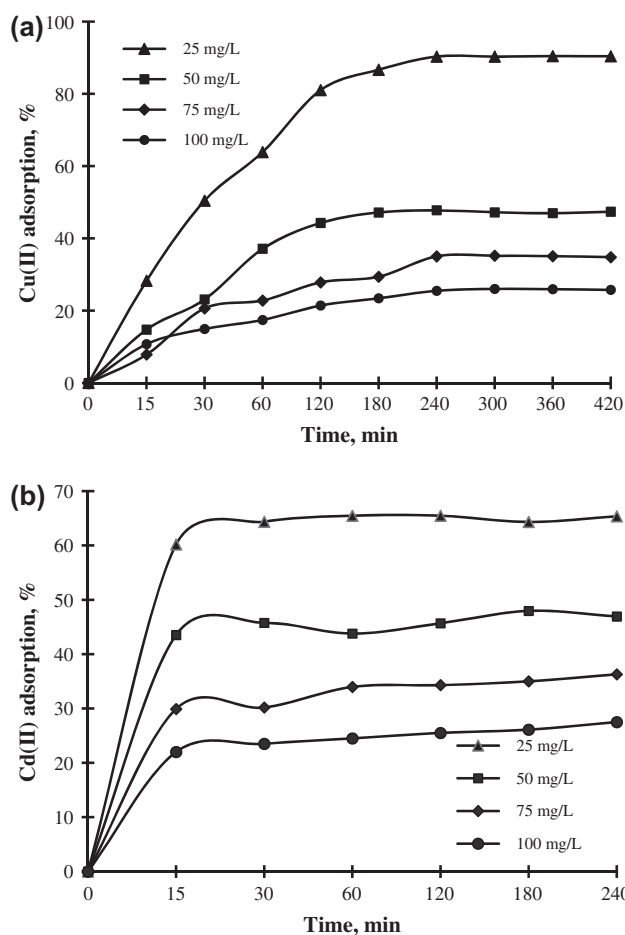


Fig. 2. Effect of time and initial concentration on (a) Cu(II) and (b) Cd(II) adsorption on *w*MNR. Conditions: pH: 5.5, Temp.: 303 K, *w*MNR: 1 g L^{-1} .

determined as 6.5. Detailed infra red spectra and XRD of *w*MNR has been described previously [27]. The X-ray diffraction patterns of air-dried MNR and *w*MNR showed MnCO_3 , Mn_2SiO_4 , and $\text{Mn}_2\text{SiO}_3(\text{OH})_2 \cdot \text{H}_2\text{O}$ as major phases. Washing of MNR did not affect the positions of the characteristic peaks of above phases. IR spectra of MNR showed absorption bands attributed to $\nu(\text{C}-\text{O})$ and $\delta(\text{OCO})$ vibrations, O–H stretching, and vibration bending modes. These bands remained unchanged after washing of MNR. However, absorption band assigned to ammonia and sulfate was absent in *w*MNR due to removal in washing with water.

3.2. Effect of time and initial concentration on adsorption

Metal ion uptake capacities were determined as a function of time to determine an optimum contact time for the adsorption of heavy metal ions on *w*MNR. The time course of adsorption of Cu(II) and Cd(II) on *w*MNR at varying initial concentrations is given in Fig. 2(a) and (b), respectively. The percentage adsorption of both the metal ions decreased with increasing initial concentration of respective metal ion. This was presumably due to the reason that numbers of available site for adsorption are always limited for a fixed dose of *w*MNR. Although the percentage of Cu(II) and Cd(II) adsorption decreased with increase of its initial concentration, the overall uptake increased progressively. The cadmium adsorption was found relatively fast and more than 85–90% of the total adsorption took place within 15 min and thereafter, it slowed down to attain the equilibrium at ~30 min. On the other hand, adsorption of Cu(II) onto *w*MNR increased progressively up to 240 min and attained the equilibrium. The Cu(II) removal at equilibrium was 90, 48, 35, and 26%, for initial Cu(II) concentration of 25, 50, 75, and 100 mg L⁻¹, respectively. The Cd(II) removal at equilibrium was 64, 46, 30, and 34% for 25, 50, 75, and 100 mg L⁻¹ initial Cd²⁺ ions, respectively. The faster adsorption of Cd(II) than Cu(II) under identical conditions (pH ~ 5.5) is also partly due to better interaction between the adsorbent surface and Cd(II). The relatively high adsorption rate of Cd(II) with lower equilibrium time also indicated greater practical importance than that for Cu(II) adsorption onto *w*MNR and may be favorable in column or continuous operation, where the contact time between the metal solution and the sorbent has been generally short. Some of the other systems have been reported to have equilibrium achieved between 2 and 72 h [28–30]. The short equilibrium

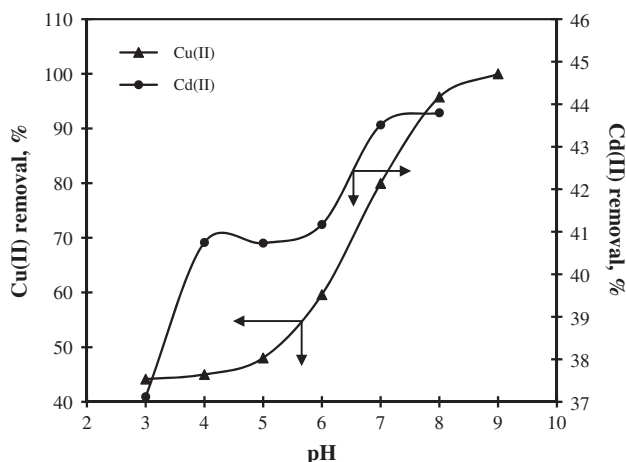


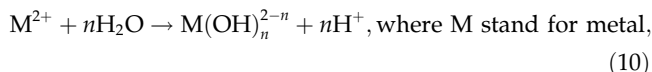
Fig. 3. Effect of solution pH on Cu(II) and Cd(II) adsorption on *w*MNR. Conditions: C_0 : 50 mg L⁻¹, temp.: 303 K, time: 240 min for Cu(II) and 60 min for Cd(II), *w*MNR: 1 g L⁻¹.

adsorption time between 15 and 30 min has been reported for polyethylene-coated silica gel and ligand-modified gel beads [31,32]. Even shorter equilibrium time 2–10 min obtained when sawdust was employed in the removal of Cd(II) ions [33,34].

3.3. Effect of pH

The pH of solution is an important parameter, which strongly affects the adsorption of heavy metal ions. The adsorption of Cu(II) and Cd(II) was studied over the range of pH 3–8 and the results are shown in Fig. 3. It was seen that adsorption of both the metal ions increased with the pH of solution, which might be partly attributed to the formation of different hydroxo species with rise in solution pH.

Based on the hydrolysis constants [35,36] of different metal ions as defined in Eq. (10).



The Cu(II) speciation reported by Das and Jana [14] showed that the dominant Cu(II) species up to pH 6.0 was Cu^{2+} . The $\text{Cu}(\text{OH})^+$ was 40% abundant in pH range 6–8, whereas dominating Cu(II) species at pH >8.0 was $\text{Cu}(\text{OH})_2$. In case of cadmium, dominant Cd(II) species up to pH 7.5 was Cd^{2+} . The $\text{Cd}(\text{OH})_2$ exist at pH >9.5 and $\text{Cd}(\text{OH})^+$ exist between pH range 7.5 and 9.5 [14]. Therefore, it may safely be stated that the removal of copper and cadmium up to pH ~8 and pH ~9.5 should be only due to adsorption and not

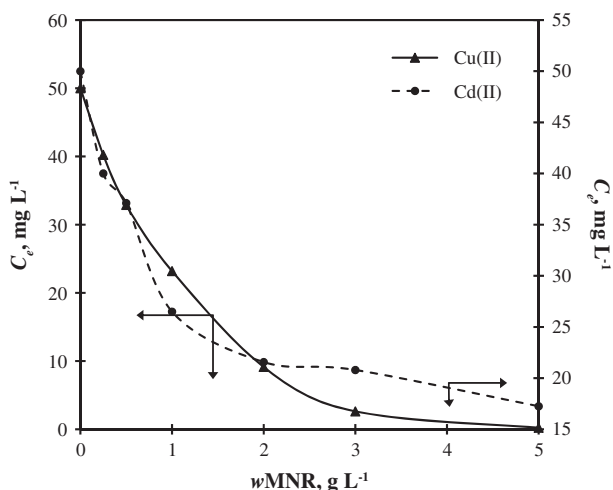


Fig. 4. Effect of $wMNR$ dose on Cu(II) and Cd(II) equilibrium concentration after adsorption. Conditions: C_0 : 50 mg L^{-1} , pH: 5.5, temp.: 303 K, time: 240 min for Cu(II) and 60 min for Cd(II).

precipitation. At low pH values, the concentration of H_3O^+ far exceeded that of adsorbate metal ions and hence, H_3O^+ ions occupied the surface binding sites, leaving Cu(II) and Cd(II) ions free in solution. This caused a competition effect between the H_3O^+ ions

and adsorbate metal ions for adsorption at lower pH. As the pH increased, the competing effect of H_3O^+ ions decreased and the positively charged ions (Cu^{2+} and $Cu(OH)^+$ ions of copper and Cd^{2+} and $Cd(OH)^+$ ions of cadmium) adhered to the free binding sites. Hence, the metal uptake was increased with the increase in pH of solution.

The other important factor, which might contribute to the higher adsorption of metal ions with increased pH, was the pH_{pzc} of $wMNR$ i.e. 6.5. At any pH below pH_{pzc} , the surface of metal oxides/oxyhydroxides has been positively charged and at pH above pH_{pzc} , the surface has been negative [17]. When the solution pH exceeded pH_{pzc} (>6.5), the metal species were more easily attracted by the negatively charged surface of adsorbent, favoring accumulation of metal species on the surface and thus promoted adsorption.

3.4. Effect of adsorbent dose

Adsorption of 50 mg L^{-1} Cu(II) or Cd(II) with different $wMNR$ doses ($0.25\text{--}5.0\text{ g L}^{-1}$) was carried out to assess its metal removal efficiency towards copper and cadmium, which is depicted in Fig. 4.

The results showed that the equilibrium concentration (C_e) of Cu(II) decreased with increase in the weight

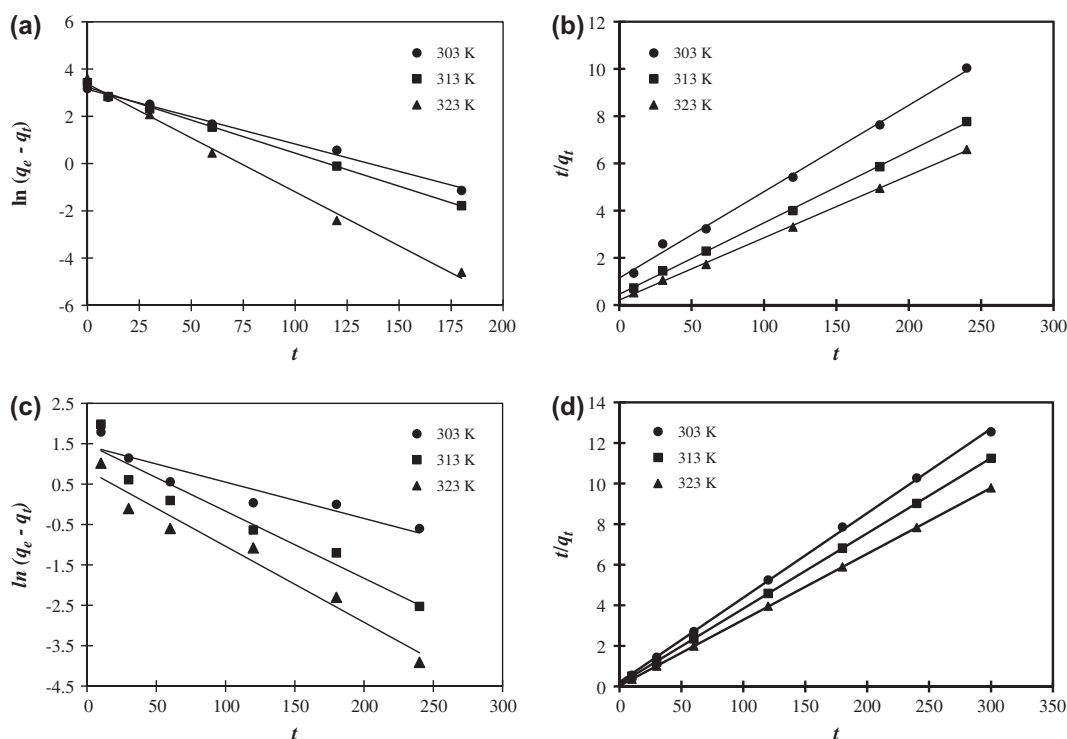


Fig. 5. Kinetic plots: (a) Pseudo-first-order model and (b) Pseudo-second-order model for Cu(II) adsorption onto $wMNR$; (c) Pseudo-first-order model and (d) Pseudo-second-order model for Cd(II) adsorption onto $wMNR$.

of $wMNR$, which was 40 mg L^{-1} for 0.25 g L^{-1} of $wMNR$ but only 0.2 mg L^{-1} for 5.0 g L^{-1} of $wMNR$ was observed. This might be due to reason that increase of $wMNR$ dose provided higher surface area and active sites for adsorption of more uptake of Cu(II) and Cd (II). However, Cd(II) concentration could be decreased only to 17.25 mg L^{-1} from initial concentration of 50 mg L^{-1} with 5.0 g L^{-1} $wMNR$ addition, which presumably required higher dose of $wMNR$ for complete removal.

3.5. Adsorption kinetics

Kinetic studies were done at three temperatures (303, 313, and 323 K) with initial Cu(II) and Cd(II) concentration of 50 mg L^{-1} in a separate set of experiments. Plots of $\log(q_e - q_t)$ vs. t i.e. pseudo-first-order and t/q_t vs. t i.e. pseudo-second-order model for $C_o = 50 \text{ mg L}^{-1}$ are shown in Fig. 5(a) and (b), respectively, for Cu(II) adsorption kinetics. The Cd(II) adsorption kinetics is depicted in Fig. 5(c) and (d) for pseudo-first-order and pseudo-second-order models, respectively. A linear relationship was apparent from Fig. 5(a)–(d) in Cu(II) and Cd(II) adsorption kinetics for both the models. The rate constants and other parameters for adsorption of Cu(II) and Cd(II) were calculated using model equations (Eqs. (2) and (3)), given in Tables 3 and 4, respectively. A closer look on regression coefficient values revealed that pseudo-second-order model fitted better with the kinetics data for both the cations. In addition, the good agreement between model fit and experimentally observed equilibrium adsorption capacity suggested that Cu(II) and

Cd(II) adsorption followed pseudo-second-order kinetics and Cu(II) or Cd(II) ions were adsorbed onto the $wMNR$ surface via chemical interaction. The pseudo-second-order model was also found applicable when acid-treated leached manganese nodule residues were used for Cu(II) and Cd(II) adsorption from their aqueous solution [37,38].

The adsorption kinetics at different initial concentrations of metal ions and temperatures, listed in Tables 3 and 4, also showed that the initial sorption rate correlated positively with the temperature. For example, at initial Cu(II) of 50 mg L^{-1} , the initial sorption rate increased from 0.87 to $4.74 \text{ mg g}^{-1} \text{ min}^{-1}$ when solution temperatures was changed from 303 to 323 K . Analogous trend was seen with the rate constants. The equilibrium sorption capacity was increased with temperature indicating endothermic nature of adsorption. It was interesting to note that value of rate constant (k_2) at particular temperature for Cd(II) rose by factor of 2 when C_o was doubled. However, this was valid for $C_o \leq 50 \text{ mg L}^{-1}$. It was also notable that for each 10 degrees increment of solution temperature, at fixed C_o of Cd(II), the k_2 increased by factor of $1^{1/2}$ – 2 .

The intraparticle diffusion often plays important role in adsorption process when adsorbent is porous materials [39]. Therefore, kinetics data was fitted into intraparticle diffusion model using Eq. (4). Plots of q_t vs. $t^{1/2}$ for Cu(II) and Cd(II) are shown in Fig. 6(a) and (b), respectively. Each curve in Figs. 6(a) and 6(b) comprised three distinct sections: initial curved or steep-sloped portion represents the bulk diffusion or exterior adsorption rate which is very high, the

Table 3
Adsorption kinetic model rate constants for Cu(II) adsorption on $wMNR$ at different temperatures

Temp. (K)	C_o (mg L^{-1})	q_e exp. (mg g^{-1})	Pseudo first-order			Pseudo second-order			
			k_1 (min^{-1})	q_e cal. (mg g^{-1})	r_1^2	k_2 ($\text{g mg}^{-1} \text{ min}^{-1}$)	q_e cal. (mg g^{-1})	h ($\text{mg g}^{-1} \text{ min}^{-1}$)	r_2^2
303	25	22.58	0.017	19.02	0.992	0.0013	25.32	0.85	0.999
	50	23.90	0.023	23.15	0.994	0.0011	27.78	0.87	0.996
	75	26.27	0.009	19.57	0.887	0.0009	29.41	0.76	0.977
	100	25.50	0.012	18.60	0.961	0.0014	27.78	1.05	0.992
313	25	24.11	0.026	15.51	0.976	0.0040	25.19	2.54	1.000
	50	30.87	0.028	25.45	0.997	0.0019	33.33	2.19	0.999
	75	32.46	0.014	21.48	0.953	0.0016	34.48	1.89	0.993
	100	21.01	0.013	22.51	0.954	0.0012	34.48	1.48	0.993
323	25	24.38	0.047	20.96	0.985	0.0044	25.57	2.89	0.999
	50	26.41	0.045	29.14	0.994	0.0032	28.46	4.74	0.999
	75	40.13	0.028	24.58	0.961	0.0028	43.47	4.42	0.999
	100	41.13	0.016	29.17	0.964	0.0011	45.45	2.20	0.997

Table 4
Adsorption kinetic model rate constants for Cd²⁺ adsorption on *w*MNR at different temperatures

Temp. (K)	C _o (mg L ⁻¹)	q _e exp. (mg g ⁻¹)	Pseudo first-order			Pseudo second-order			
			k ₁ (min ⁻¹)	q _e cal. (mg g ⁻¹)	r ₁ ²	k ₂ (g mg ⁻¹ min ⁻¹)	q _e cal. (mg g ⁻¹)	h (mg g ⁻¹ min ⁻¹)	r ₂ ²
303	25	17.01	0.006	5.84	0.978	0.0039	17.15	1.17	0.994
	50	23.90	0.009	4.25	0.851	0.0079	24.04	1.60	0.999
	75	30.00	0.006	16.31	0.767	0.0016	29.85	1.42	0.992
	100	31.60	0.006	17.79	0.681	0.0037	27.10	2.72	0.998
313	25	18.86	0.020	6.35	0.985	0.0079	19.31	2.94	0.999
	50	26.68	0.016	4.45	0.923	0.011	26.95	7.92	1.000
	75	33.5	0.012	11.15	0.745	0.0049	33.73	5.59	0.999
	100	31.05	0.013	11.73	0.738	0.0073	30.40	6.76	0.999
323	25	20.75	0.023	3.7	0.923	0.013	20.96	7.16	0.999
	50	30.65	0.018	6.33	0.959	0.026	30.77	24.81	1.000
	75	36.79	0.025	11.93	0.861	0.0062	37.45	8.81	0.999
	100	36.45	0.031	11.30	0.799	0.019	36.69	24.69	1.000

subsequent linear portion is attributed to the intraparticle diffusion, and plateau portion represents the equilibrium [23,40]. The intraparticle diffusion constants were calculated from the slopes of the linear portions of the curves for both the cations and given in Table 5. The value of the intercept C in the second section provided information related to the thickness of the boundary layer [23]. The increasing values of intercept values increased with the temperature suggest importance of surface diffusion at high temperatures, which is presumably due to the greater random motion associated with the increased thermal energy. Although, linear section supported involvement of intraparticle diffusion in Cu(II) and Cd(II) adsorption onto *w*MNR, deviation of curve from origin indicated role of another rate-limiting steps. In addition, multilinearity (like in present case) in curves drawn between q_t and $t^{0.5}$ has been often attributed to involvement of two or more steps in adsorption kinetics [40,41].

3.6. Adsorption activation energy

The effect of temperature on adsorption of cations i.e. Cu(II) and Cd(II) on *w*MNR was further evaluated using Arrhenius equation [23,37]. Arrhenius equation parameters were fitted using pseudo-second-order rate constants to determine temperature-independent rate parameters and adsorption type using equation expressed in Eq. (11) as:

$$k_2 = k \times e^{\left(-\frac{E_a}{RT}\right)} \quad (11)$$

where k is the temperature-independent factor (g mg⁻¹ h⁻¹), E_a the activation energy of sorption (kJ mol⁻¹), R the universal gas constant (8.314 J mol⁻¹ K), and T the solution temperature (K). Plots of $\ln k_2$ vs. $1/T$ yielded straight line, with slope $-E_a/R$ for both the cations at different initial concentrations, which is shown in Fig. 7(a)–(b) for $C_o = 50$ mg L⁻¹ for both the cations. The magnitude of the activation energy has been commonly used as the basis for differentiating between physical and chemical adsorption. Physical adsorption reactions have been readily reversible, equilibrium attained rapidly, and thus energy requirements have been small, ranging from 5 to 40 kJ mol⁻¹. On the other hand, chemical adsorption has been specific, involves stronger forces, and thus requires larger activation energies (e.g. 40–800 kJ mol⁻¹) [40,42]. The activation energy for Cu(II) and Cd(II) adsorption onto *w*MNR was found to be 40–50 and 50.76–65.14 kJ mol⁻¹, respectively, for different initial concentrations. This suggested possible role of chemical exchange/interaction during Cu(II) and Cd(II) ions adsorption onto the *w*MNR surface.

3.7. Adsorption isotherm studies

The equilibrium data was fitted into the linearized form of Langmuir and Freundlich models shown in Eqs. (5) and (6), respectively. The Langmuir plot of C_e vs. C_e/q_e and Freundlich plot of $\ln q_e$ vs. $\ln C_e$ were drawn, which were found to be linear for both Cu(II) and Cd(II). The derived parameters from least-squares fittings of the Langmuir and Freundlich equations are given in Table 6. The adsorption equilibrium data of Cu(II) and Cd(II) fitted better with the Langmuir

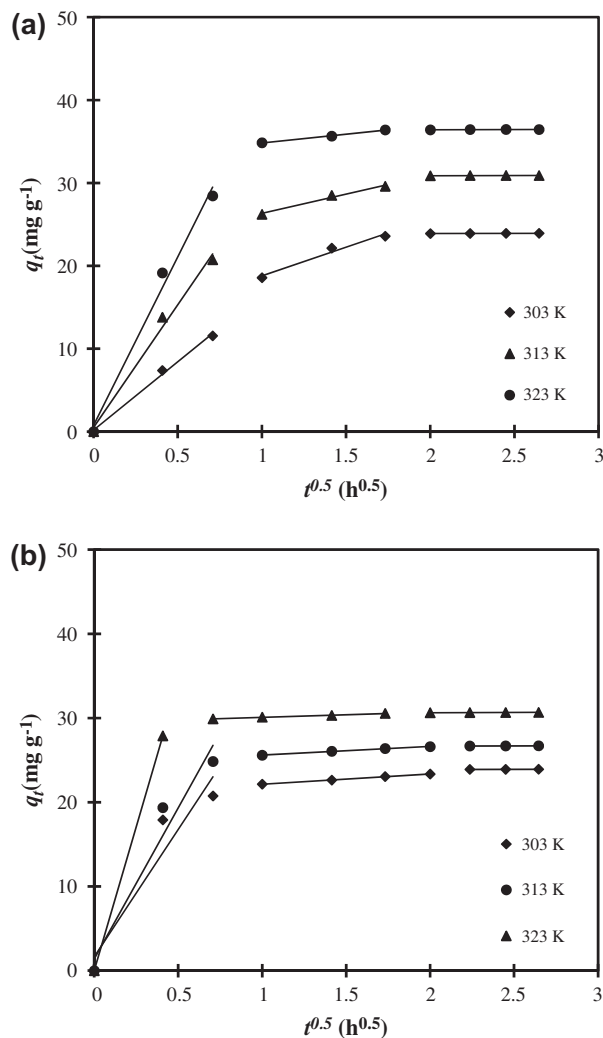


Fig. 6. Intraparticle diffusion plots for (a) Cu^{2+} and (b) Cd^{2+} adsorption onto *w*MNR.

model in comparison to the Freundlich model as evident from r^2 values in Table 6. To determine whether the adsorption process was favorable or unfavorable, the value of R_L constant was calculated, which has been described as a dimensionless constant separation factor [37], where $R_L > 1$ unfavorable; $R_L = 1$ linear;

$0 < R_L < 1$ favourable; and $R_L = 0$ irreversible. The value of R_L was calculated using the Eq. (12).

$$R_L = \frac{1}{1 + bC_o} \quad (12)$$

where C_o was the initial metal concentration (mg L^{-1}) and b is the Langmuir parameter i.e. energy of interaction at the surface. The calculated values of R_L were found in the range 0.135–0.004 showing favorable adsorption of $\text{Cu}(\text{II})$ on *w*MNR. The value of R_L as function of initial $\text{Cu}(\text{II})$ concentrations at different temperatures were plotted in Fig. 8, which showed that favorability of adsorption increased with increasing concentration of $\text{Cu}(\text{II})$ at certain temperature. Besides, increasing temperature also enhanced the favorability in terms of R_L value for a certain concentration of $\text{Cu}(\text{II})$ in the solution. Similar trends were seen for $\text{Cd}(\text{II})$ adsorption equilibrium data at different initial concentrations.

3.8. Thermodynamic studies

Thermodynamic parameters for $\text{Cu}(\text{II})$ adsorption were quantified to increase the utility of measured equilibrium and kinetics data. The thermodynamic parameters were determined from the thermodynamic equilibrium constant, K_d (or the thermodynamic distribution coefficient). The standard Gibbs free energy ΔG° (kJ mol^{-1}), standard enthalpy change ΔH° (kJ mol^{-1}), and standard entropy change ΔS° ($\text{J mol}^{-1} \text{K}^{-1}$) were calculated using the Eqs. (7), (8), and (9). K_d at different temperatures was determined by plotting $\ln(C_s/C_e)$ vs. C_s (Fig. 9(a)) and extrapolating C_s to zero [23,24]. $\ln K_d$ was plotted against $1/T$ to calculate ΔH° and ΔS° from the slope and intercept, respectively (Fig. 9b) [23,25], which has been given in Table 7 along with Gibbs free energy (ΔG°) of adsorption. Negative values of ΔG° indicated spontaneous adsorption and increased degree of spontaneity of the reaction with the temperature. The positive standard enthalpy change for the present study confirmed endothermic nature of $\text{Cu}(\text{II})$ and $\text{Cd}(\text{II})$ adsorption

Table 5

Intraparticle diffusion coefficients and intercept values for $\text{Cu}(\text{II})$ and $\text{Cd}(\text{II})$ adsorption on *w*MNR at different temperatures

Temp. (K)	Cu(II)			Cd(II)		
	K_{id} ($\text{mg g}^{-1} \text{h}^{0.5}$)	Intercept (C)	r^2	K_{id} ($\text{mg g}^{-1} \text{h}^{0.5}$)	Intercept (C)	r^2
303	6.931	11.85	0.973	1.211	20.93	0.999
313	4.661	21.66	0.984	1.028	24.57	0.995
323	2.108	32.72	0.996	0.616	29.46	0.994

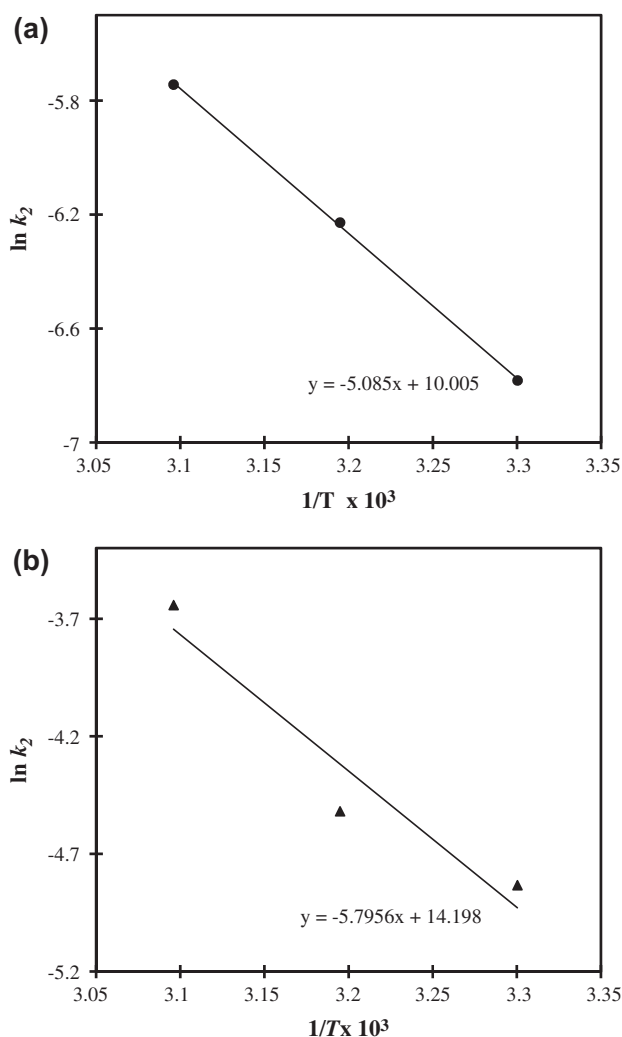


Fig. 7. Determination of the activation energy for (a) Cu^{2+} and (b) Cd^{2+} adsorption on *wMNR*.

onto *wMNR*. The positive ΔS° suggested the increasing randomness at the solid–solution interface during

the adsorption of copper or cadmium on *wMNR* and reflects the affinity of the *wMNR* towards adsorbate metal ion [23].

3.9. Loading capacity

The influence of varying amount of Cu^{2+} and Cd^{2+} concentration and adsorbent dose at $\text{pH} \sim 5.5 \pm 0.2$ have been shown in Figs. 2 and 4, respectively. The 5 g L^{-1} *wMNR* was sufficient for complete adsorption of copper from an initial Cu^{2+} concentration of 50 mg L^{-1} (Fig. 4). At any particular level of Cu^{2+} adsorption (say 90%), the loading capacity was found to be dependent on initial copper concentration. It was found that the loading capacity increased with initial metal ion concentration; for example, in Cu(II) adsorption, it reached to a maximum value of $\sim 27 \text{ mg g}^{-1}$ with initial Cu^{2+} of 75 mg L^{-1} and then marginally decreased. The Q^o i.e. maximum loading capacity value for Cu and Cd adsorption on this adsorbent as determined by Langmuir isotherm data was found to be 26.95 and 32.26 mg g^{-1} , respectively, at 303 K (Table 5). Analogous trends are obtained for Cd^{2+} adsorption onto *wMNR*. The loading capacities of some adsorbents and *wMNR* for the removal of Cu^{2+} and Cd^{2+} are given in Table 8 for comparison. For copper uptake, the *wMNR* had a greater capacity than peat [43], comparable to electric furnace slag [44] and manganese nodules [45] and slightly lower to calcined phosphate rock [46]. The temperature positively affected the loading of Cu^{2+} onto *wMNR* as the loading capacity of 26.95 mg g^{-1} at 303 K improved to 32.36 mg g^{-1} at 313 K and up to 40.32 mg g^{-1} at 323 K. Thus, promising improvement in Cu^{2+} sorption by *wMNR* has been achieved by raising the temperature while treating the Cu containing aqueous solutions.

Table 6
Isotherm parameters for Cu(II) and Cd(II) adsorption onto *wMNR*

Adsorbate metal ion	Temp. (K)	Langmuir isotherm			Freundlich isotherm		
		Adsorption maxima Q^o (mg g^{-1})	Binding energy constant b (mg L^{-1}) $^{-1}$	Regression coefficient r^2	Adsorption capacity K_f (mg g^{-1})	Adsorption intensity $1/n$	Regression coefficient r^2
Cu(II)	303	26.95	1.28	0.999	12.42	0.21	0.914
	313	32.36	2.41	0.999	14.93	0.22	0.939
	323	40.32	2.82	0.999	20.04	0.16	0.985
Cd(II)	303	32.26	0.258	0.981	10.52	0.26	0.973
	313	35.97	0.335	0.984	14.68	0.21	0.989
	323	38.17	0.562	0.994	18.61	0.17	0.973

3.10. Desorption studies

The success of an adsorbent lies in its regeneration (by desorption) for potential commercial application. Desorption study also help to elucidate the nature of the adsorption process. Desorption/regeneration experiments were carried out by treating 0.1 g adsorbent loaded with copper or cadmium ions under optimized conditions (pH \sim 5.5, 50 mgL⁻¹ initial concentration of metal ion) with 100 mL deionised water adjusted to various pH values in the range 2.0–7.0 using an aqueous HNO₃ and NaOH solution, and then mechanically stirred for 2 h at room temperature. The solid adsorbent was then separated by centrifugation and the concentration of desorbed copper or cadmium ions in the solution was determined spectrophotometrically. The percentage of desorption of Cu(II) from *w*MNR was almost 90% at pH 2.0, which decreased with increase in pH. The desorption percentages of Cu(II) obtained at pH 3, 4, and 5 were 52, 24, and 10%, respectively. Beyond a pH of 5.0, the percentage of desorption was negligible. The desorption of Cd²⁺ at pH 2, 3, 4, and 5 were 80, 29.22, 11.59, and 3.09%, respectively. The equilibrium Cd²⁺ after desorption experiment was found to decrease after pH 5. The desorption of Cu(II) and Cd(II) showed that *w*MNR can be regenerated after removal of Cu(II) from aqueous acidic solution and can be reused for further adsorption. The regeneration of *w*MNR also indicated that adsorption of Cu(II) or Cd(II) on to the *w*MNR was a reversible process.

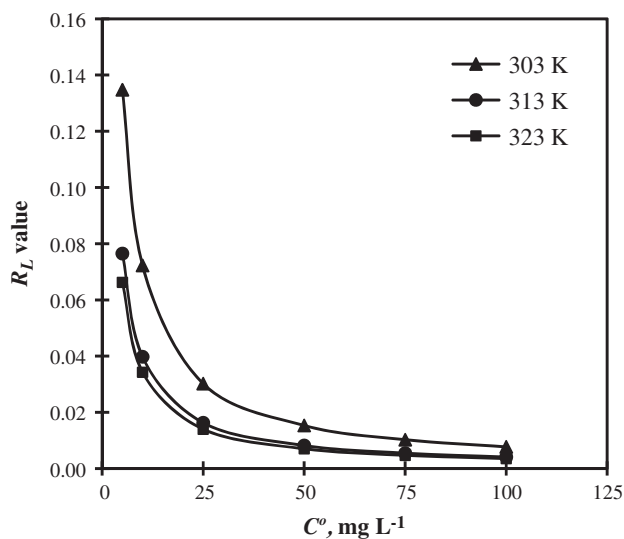


Fig. 8. Effect of temperature and initial Cu(II) concentration on the separation factor (R_L).

3.11. Mechanism of Cu²⁺ and Cd²⁺ sorption onto *w*MNR

The adsorption of heavy metals onto adsorbent surfaces can involve various mechanisms such as electrostatic attraction/repulsion, chemical interaction, and ligand exchange. The adsorption mechanisms are often deduced from sorption kinetics and equilibrium data. Faster kinetics, like in present case, has been attributed to chemical interaction/ion exchange mechanism of sorption. As apparent from Tables 3 and 4, sorption of Cd²⁺ and Cu²⁺ onto *w*MNR follows pseudo-second-order kinetics, indicating chemical interaction between adsorbent and adsorbate during sorption. However, it may not be rate controlling step for the Cd²⁺ sorption onto *w*MNR due to rapid rate of uptake. ΔH° between 5.0 and 100 kcal mol⁻¹ (20.9–418.4 kJ mol⁻¹) has been reported as energy of chemi-

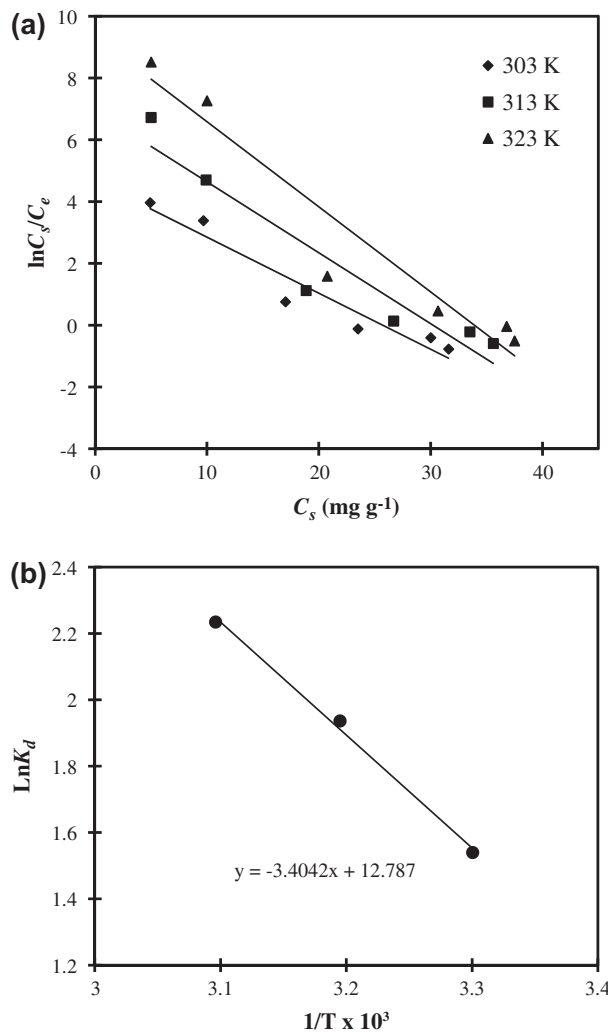


Fig. 9. Illustrations of (a) Determination of thermodynamic distribution coefficient and (b) Plot K_d vs. $1/T$, for Cd(II) adsorption onto *w*MNR.

Table 7
Thermodynamic parameters obtained from Cu(II) and Cd(II) adsorption onto *w*MNR

Metal ion	Temp. (K)	K_d	ΔG° (kJ mol ⁻¹)	ΔH° (kJ mol ⁻¹)	ΔS° (J mol ⁻¹ K ⁻¹)
Cu(II)	303	4.711	-3.90	34.91	127.87
	313	6.825	-5.00		
	323	11.13	-6.47		
Cd(II)	303	4.66	-3.88	28.3	106.25
	313	6.99	-5.04		
	323	9.34	-6.00		

Table 8
Comparative adsorption capacity of some adsorbents for Cu(II) and Cd(II) ions

Adsorbents	pH	Initial metal ion concentration (mg L ⁻¹)	Adsorption capacity (mg g ⁻¹)	References
Peat	4.5	10–150	12.48 (Cu ²⁺)	[43]
Electric furnace slag	4.5	100–1,000	26.2 (Cu ²⁺)	[44]
Natural clinoptilolite	–	10–185	2.95–12.0 (Cu ²⁺)	[47]
	–	10–125	3.37–14.1 (Cd ²⁺)	
Bagasse flyash	6.0	2–20	1.24 (Cd ²⁺)	[48]
Hematite	9.2	71.15	0.227 (Cd ²⁺)	[49]
Manganese nodules	4.0	6.4–38.1	26.0 (Cu ²⁺)	[45]
Calcined phosphate rock	5.0	10–150	32.15 (Cu ²⁺)	[46]
IMMT-MNR ^a	6.0	9.4–100	25.4 (Cu ²⁺)	[14]
	6.0	9.3–100	18.7 (Cd ²⁺)	
AT-MNR ^b	–	100–500	19.65 (Cu ²⁺)	[37,38]
	–	200–500	19.80 (Cd ²⁺)	
<i>w</i> MNR	5.5	5–100	26.95 (Cu ²⁺)	Present work
	5.5	5–100	32.26 (Cd ²⁺)	

^aManganese nodule residue generated through IMMT process.

^bAcid treated manganese nodule residue.

cal reaction comparable to adsorption taking place by chemical reaction i.e. chemisorption [39]. The ΔH° value obtained in present work (34.91 and 28.3 kJ mol⁻¹) indicated chemisorption-type uptake of Cu²⁺ and Cd²⁺ on *w*MNR. In addition to this, values of energy of activation (50.76–65.14 kJ mol⁻¹ for Cu²⁺ and 50.76–65.14 kJ mol⁻¹ for Cd²⁺) for temperature range 303–323 K also supported the chemical interaction between metal ions and *w*MNR surface. The equilibrium sorption capacity increased with temperature also indicated involvement of chemical reactions as well as diffusion-based interaction between adsorbate and adsorbent during adsorption [40,50]. The adsorption process on porous sorbents has been generally described with four stages, and one or more of which may determine the rate of adsorption and amount of adsorption on the solid surface. Those stages are described as bulk diffusion, film diffusion, intraparticle diffusion, and finally adsorption of the

solute on the surface [51]. Generally, bulk diffusion and adsorption steps are assumed to be rapid and, therefore, not rate determining. The adsorbent used in present studies (*w*MNR) had extensive range of pore sizes (0.36–106 nm) including micro-, meso-, and macropores. In addition, macropores are usually hydrated in the aqueous system and may act as meso- or micro-pores. This type of material gave rise to three stage plot of q_t vs. $t^{1/2}$, as shown in Fig. 8, which comprised three distinct sections: initial plot or steep-sloped portion represents the bulk diffusion or exterior adsorption rate which is very high, the subsequent linear portion is attributed to the intraparticle diffusion, and plateau portion represents the equilibrium [23]. The value of the intercept C in this second section of Fig. 8 also provided information related to the thickness of the boundary layer [52]. The increasing values of intercept values with the rise in temperature suggested importance of surface diffusion at

elevated temperatures (Table 4), which was presumably, due to the greater random motion associated with the increased thermal energy. Although linear section supports involvement of intraparticle diffusion in Cd^{2+} adsorption onto *w*MNR, deviation of curve from origin indicated role of another rate-limiting steps. The multilinearity (like in present case) in curves drawn between q_t and t has been often attributed to involvement of two or more steps in adsorption kinetics [40,41]. Thus, it may be concluded that sorption of Cd^{2+} and Cu^{2+} on to *w*MNR take place via chemical interaction at interface occurring under diffusion gradient throughout the porous surface of leached manganese nodule residue.

4. Conclusions

The leached manganese nodule residue generated by reduction roast-ammonia leaching has been shown to be a potentially useful material for removal of copper and cadmium from aqueous solution. The equilibrium was attained in 240 and 30 min for Cu(II) and Cd(II), respectively, irrespective of their initial concentration in the solution. Comparison of regression coefficient values showed that the adsorption of Cu(II) and Cd(II) on leached manganese nodule residue followed pseudo-second-order kinetics. The values of activation energy indicated chemisorption of Cu(II) and Cd(II) onto *w*MNR. The kinetic rate constants and loading capacity of *w*MNR increased with increasing temperature indicated endothermic nature of adsorption reactions. About 80–90% desorption of Cu(II) and Cd(II) could be achieved at pH range 2–4. The adsorption data fitted well into the Langmuir isotherm. The separation (R_L) value calculated from isotherm data depicted favorable adsorption of copper. The Q^o i.e. maximum loading capacity value for Cu(II) adsorption on this adsorbent was found to be temperature-dependent, which was 26.95 mg g^{-1} at 303 K and improved to 40.32 mg g^{-1} at 323 K. The Q^o i.e. Langmuir maximum loading capacity value for Cd(II) adsorption was found to be 32.23 mg g^{-1} at 303 K, improving to 38.14 mg g^{-1} at 323 K. Thus, absorption properties of leached manganese nodule residue can be utilized for treatment of industrial effluents to bring down the high Cu and Cd metal to the level suitable for its safe disposal in inland water bodies.

References

- [1] M. Hanaa, S. Eweida, A. Eweida, A. Farag, Heavy metals in drinking water and their environmental impact on human health, in: ICEHM2000, Cairo University, Egypt, 2000, pp. 542–556.
- [2] F. Rozada, M. Otero, A. Moran, A.I. García, Adsorption of heavy metals onto sewage sludge-derived materials, *Biore-sour. Technol.* 99 (2008) 6332–6338.
- [3] C.R. Evanko, D.A. Dzombak, Remediation of metal contaminated soils and waste water (Technology Evaluation Report), in: Ground-Water Remediation Technologies Analysis Center (GWRAC), Concurrent Technologies Corporation, Pittsburgh, PA, US, 1997.
- [4] Indian Standards Institution, Tolerance Limits for Industrial Effluents: ISI 2490 (Part I), Bureau of Indian Standards, India, 1981.
- [5] Indian Standards Institution, Drinking Water Specifications: IS 10500, Bureau of Indian Standards, India, 1991.
- [6] L.A. Smith, J.L. Means, A. Chen, B. Alleman, C.C. Chapman, J.S. Tixier, Jr., S.E. Brauning, A.R. Gavaskar, M.D. Royer, Remedial Options for Metals-contaminated Sites, Lewis Publishers, Boca Raton, FL, 1995.
- [7] N.K. Lazaridis, E.N. Peleka, Th.D. Karapantsios, K.A. Matis, Copper removal from effluents by various separation techniques, *Hydrometallurgy* 74 (2004) 149–156.
- [8] K.S. Rao, M. Mohapatra, S. Anand, P. Venkateswarlu, Review on cadmium removal from aqueous solutions, *Int. J. Eng. Sci. Technol.* 2 (2010) 81–103.
- [9] N.L.D. Filho, Y. Gushiken, W.L. Polito, J.C. Moreiza, Sorption and preconcentrations of metal ions in ethanol solutions with silica gel modified with benzimidazole, *Talanta* 42 (1995) 1630–1663.
- [10] C.D. Jadia, M.H. Fulekar, Phytoremediation of heavy metals: Recent techniques, *Afr. J. Biotech.* 8 (2009) 921–928.
- [11] A.F. Bertocchi, G. Marcello, P. Roberto, Z. Antonio, Red mud and fly ash for remediation of mine sites contaminated with As, Cd, Cu, Pb and Zn, *J. Hazard. Mater.* B134 (2006) 112–119.
- [12] A.L. Degodo, C. Perez, F.A. Copez, Sorption of heavy metals on blast furnace sludge, *Indian J. Chem. Technol.* 32 (1998) 1989–1996.
- [13] M. Machida, R. Yamazaki, M. Aikawa, H. Tatsumoto, Role of minerals in carbonaceous adsorbents for removal of Pb(II) ions from aqueous solution, *Sep. Purif. Technol.* 46 (2005) 88–94.
- [14] N.N. Das, R.K. Jana, Adsorption of some bivalent heavy metal ions from aqueous solutions by manganese nodule leached residues, *J. Colloid Interface Sci.* 293 (2006) 253–262.
- [15] K.M. Parida, S. Mallick, B.K. Mohapatra, V.N. Misra, Studies on manganese-nodule leached residues 1. Physicochemical characterization and its adsorption behavior toward Ni^{2+} in aqueous system, *J. Colloid Interface Sci.* 277 (2004) 48–54.
- [16] S. Mallick, S.S. Dash, K.M. Parida, Adsorption of hexavalent chromium on manganese nodule leached residue obtained from $\text{NH}_3\text{-SO}_2$ leaching, *J. Colloid Interface Sci.* 297 (2006) 419–425.
- [17] C.P. Huang, F.G. Ostavic, Removal of Cd(II) by activated carbon adsorption, *J. Environ. Eng. Div.* 104 (1978) 863–878.
- [18] Y.S. Ho, Citation review of Lagergren kinetic rate equation on adsorption reactions, *Scientometrics* 59 (2004) 171–177.
- [19] Y.S. Ho, Review of second-order models for adsorption systems, *J. Hazard. Mater.* 136 (2006) 681–689.
- [20] W.J. Weber, J.C. Moris, Advances in water pollution research: Removal of biologically-resistant pollutants from waste waters by adsorption, in: Proceedings of the First International Conference on Water Pollution Research, vol. 2, Pergamon Press, Oxford, 1962, pp. 231–266.
- [21] I. Langmuir, The constitution and fundamental properties of solids and liquids, *J. Am. Chem. Soc.* 38 (1916) 2221–2295.
- [22] H.M.F. Freundlich, Over the adsorption in solution, *J. Phys. Chem.* 57 (1906) 385–471.
- [23] H.K. Boparai, M. Joseph, D.M. O'Carroll, Kinetics and thermodynamics of cadmium ion removal by adsorption onto nanozerovalent iron particles, *J. Hazard. Mater.* 186 (2011) 458–465.

- [24] R. Calvet, Adsorption of organic-chemicals in soils, *Environ. Health Perspect.* 83 (1989) 145–177.
- [25] C. Raji, T.S. Anirudhan, Batch Cr(VI) removal by polyacrylamide-grafted saw-dust: Kinetics and thermodynamics, *Water Res.* 32 (1998) 3772–3780.
- [26] N.S. Randhawa, N.N. Das, R.K. Jana, Selenite adsorption using leached residues generated by reduction roasting-ammonia leaching of manganese nodules, *J. Hazard. Mater.* 241–242 (2012) 486–492.
- [27] R.K. Behera, P.K. Satapathy, N.S. Randhawa, N.N. Das, Adsorptive removal of phosphate ions using leached sea nodule residue generated by the reduction-roasting ammoniacal leaching process, *Adsorpt. Sci. Technol.* 28 (2010) 611–627.
- [28] N.E. Reed, M.R. Matsumoto, Modelling cadmium adsorption by activated carbon using Langmuir and Freundlich expressions, *Sep. Sci. Technol.* 28 (1993) 2179–2195.
- [29] S. Bahrami, A.S. Bassi, E. Yanful, Polyethyleneimine-containing sol-gels as novel sorbents for the removal of cadmium from aqueous solutions, *Can. J. Chem. Eng.* 77 (1999) 931–935.
- [30] C.C. Wang, C.Y. Chang, C.Y. Chen, Study on metal ion adsorption of bifunctional chelating/ion-exchange resins, *Macromol. Chem. Phys.* 202 (2001) 882–890.
- [31] M.L. Delacour, E. Gailliez, M. Bacquet, M. Morcellet, Poly (ethylene) coated onto silica gel: Adsorption capacity towards lead and mercury, *J. Appl. Polym. Sci.* 73 (1999) 899–906.
- [32] A. Denizil, S. Senel, G. Alsancak, N.T. Uzman, R. Say, Mercury removal from synthetic solutions using poly(2-hydroxyethylmethacrylate) gel beads modified with poly (ethyleneimine), *React. Funct. Polym.* 55 (2003) 121–130.
- [33] V.C. Taty-Costodes, H. Fauduet, C. Porte, A. Delacroix, Removal of Cd(II) and Pb(II) ions, from aqueous solutions, by adsorption onto sawdust of *Pinus sylvestris*, *J. Hazard. Mater.* 105 (2003) 121–142.
- [34] S.Q. Memon, N. Memon, S.W. Shah, M.Y. Khuhawar, M.I. Bhangar, Sawdust—A green and economical sorbent for the removal of cadmium (II) ions, *J. Hazard. Mater.* 139 (2007) 116–121.
- [35] D.D. Perin, B. Dempsy, Buffers for pH and Metal ion Control, Chapman & Hall, London, 1974.
- [36] A.E. Martell, R.M. Smith, Critical Stability Constants (Inorganic Chemistry), vol. IV, Plenum, New York, NY, 1977.
- [37] A. Agarwal, K.K. Sahu, B.D. Pandey, A comparative adsorption study of copper on various industrial solid wastes, *AIChE J.* 50 (2004) 2430–2438.
- [38] A. Agarwal, K.K. Sahu, Kinetic and isotherm studies of cadmium adsorption on manganese nodule residue, *J. Hazard. Mater.* B137 (2006) 915–924.
- [39] N. Unlu, M. Ersoz, Adsorption characteristics of heavy metal ions onto a low cost biopolymeric sorbent from aqueous solutions, *J. Hazard. Mater.* B136 (2006) 272–280.
- [40] F.C. Wu, R.L. Tseng, R.S. Juang, Initial behavior of intraparticle diffusion model used in the description of adsorption kinetics, *Chem. Eng. J.* 153 (2009) 1–8.
- [41] A. Ozcan, A.S. Ozcan, O. Gok, Adsorption kinetics and isotherms of anionic dye of reactive blue 19 from aqueous solutions onto DTMA-sepiolite, In: A.A. Lewinsky (Ed), *Hazardous Materials and Wastewater—Treatment, Removal and Analysis*, Nova Science Publishers, New York, NY, 2007.
- [42] E.I. Unuabonah, K.O. Adebawale, B.I. Olu-Owolabi, Kinetic and thermodynamic studies of the adsorption of lead (II) ions onto phosphate-modified kaolinite clay, *J. Hazard. Mater.* 144 (2007) 386–395.
- [43] A. Chen, C.M. Hui, G. McKay, Film-pore diffusion modeling for the sorption of metal ions from aqueous effluents onto peat, *Water Res.* 35 (2001) 3345–3356.
- [44] L. Curkovic, S.C. Stefanovic, A. Rastovean-Mioe, Batch Pb²⁺ and Cu²⁺ removal by electric furnace slag, *Water Res.* 35 (2001) 3436–3440.
- [45] K.M. Parida, P.K. Satapathy, N. Das, Studies on indian ocean manganese nodules IV. Adsorption of some bivalent heavy metal ions onto ferromanganese nodules, *J. Colloid Interface Sci.* 181 (1996) 456–462.
- [46] A. Aklil, M. Mouflih, S. Sebti, Removal of heavy metal ions from water by using calcined phosphate as a new adsorbent, *J. Hazard. Mater.* 112 (2004) 183–190.
- [47] A. Cincotti, N. Lai, R. Orru, G. Cao, Sardinian natural clinoptilolites for heavy metals and ammonium removal: Experimental and modeling, *Chem. Eng. J.* 84 (2001) 275–282.
- [48] V.K. Gupta, C.K. Jain, I. Ali, M. Sharma, V.K. Saini, Removal of cadmium and nickel from wastewater using bagasse fly ash—a sugar industry waste, *Water Res.* 37 (2003) 4038–4044.
- [49] D.B. Singh, D.O. Rupainwar, G. Prasad, K.C. Jayaprakas, Studies on the Cd(II) removal from water by adsorption, *J. Hazard. Mater.* 60 (1998) 29–40.
- [50] K.R. Hall, L.C. Eagleton, A. Acrivos, T. Vermeulen, Pore- and solid-diffusion kinetics in fixed-bed adsorption under constant pattern conditions, *Ind. Eng. Chem. Fundam.* 5 (1966) 212–223.
- [51] P. Chingombe, B. Saha, R.J. Wakeman, Sorption of atrazine on conventional and surface modified activated carbons, *J. Colloid Interface Sci.* 302 (2006) 408–416.
- [52] D. Kavitha, C. Namasivayam, Experimental and kinetic studies on methylene blue adsorption by coir pith carbon, *Bioresour. Technol.* 98 (2007) 14–21.